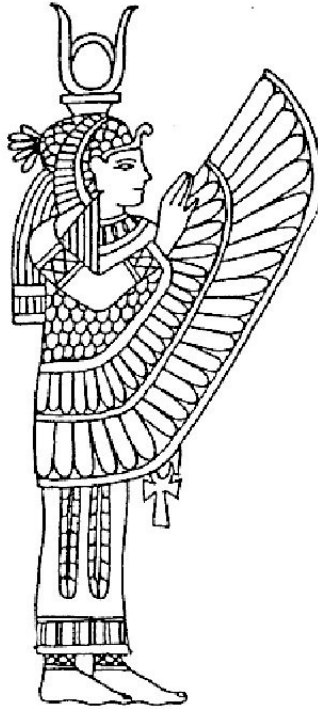


Ion Scattering Spectroscopy with a Time Of Flight System

Dotting the i's of IISIS



Author:
Hendrik Bekker

Supervisors:
Drs. Erwin Bodewits
Prof. dr. ir. Ronnie Hoekstra

Juli 2009



university of
 groningen



KVI

*atomic
physics*

Front cover: The Egyptian goddess Isis spreading her wings [8].

Contents

1. Introduction	4
1.1 IISIS	4
1.2 Surface analysis	4
2. Theory	5
2.1 Ion Scattering	5
2.2 Validity of the classical model	6
3. Experimental setup	7
3.1 Vacuum chamber	7
3.2 Deceleration	8
3.3 Time of flight	9
3.4 LEIS or LERS	9
4. Measurements	11
4.1 Deceleration	11
4.2 Ion packets	11
5. Conclusion	14
Bibliograhpy	15

1. Introduction

This report is part of the bachelor research every student of physics on the University of Groningen has to do. During a period of about 10 weeks the student learns what it means to be part of a research group. This particular thesis is the culmination of 12 weeks spend on the Inelastic Ion Surface Interaction Studies (IISIS) project.

1.1 IISIS

The IISIS setup currently resides at the Atomic Physics group (ATF) of the Kernfysisch Versneller Instituut (KVI). The GSI Helmholtz Centre for Heavy Ion Research (Darmstadt, Germany) will be the future site of the set-up. At the future HITRAP facility at GSI low-energy fully stripped ions up to U^{91+} will become available. The setup is used in a collaboration with the Atomic and Plasma Physics group of the Vienna University of Technology (TU Vienna).

The goal of the current research is to expand the knowledge on ion-induced electron emission from surfaces. This type of electron emission is important for example in plasma surface interactions as found in thermonuclear fusion reactors.

There are measurements scheduled on the effects of highly charged xenon on a gold surface, a gold surface covered with a mono-layer of C_{60} and gold covered with a bulk layer of C_{60} . The influences of the amount of kinetic energy and potential of the xenon will be measured. For that reason a separate deceleration system is installed which needs testing and configuring.

1.2 Surface analysis

When performing measurements well characterized initial conditions are of the essence, obviously when the initial conditions aren't properly characterized the results won't be optimal. For measurements on surface effects one of the important initial conditions is the amount of contamination on the surface. This makes it useful to have a means of determining the composition of the surface.

Over the past decades numerous surface analysis techniques have been developed, every one with its advantages and disadvantages [6]. For the IISIS setup a method was needed that could identify the contamination and give an indication of the amount of contamination. Ion Scattering Spectroscopy (ISS) is such a method. ISS was also chosen to be used because the implementation easily fitted in with the structural design of the IISIS setup.

At the start of the bachelor research period the necessary structural parts were already in place. The main objectives were to get familiar with ISS, the feasibility of ISS given the constraints of the IISIS setup and to get results showing correct functioning of the ISS system.

2. Theory

2.1 Ion scattering

The theory of ISS can be described by classical mechanics: atomic particles are described as if they were hard balls i.e. they undergo elastic collisions. First lets just assume this to be true and see how this can be used to gather information on the surface.

When an elastic collision takes place between two particles the result of the collision can be described by number of parameters like the total scattering angle, the velocities and the ratio of masses. Of those parameters the mass of the target atom is of interest because that is the property identifying which element it is.

Writing down the laws of energy and momentum conservation for an elastic collision gives:

$$\begin{aligned} m_p v_{i,p}^2 &= m_p v_{f,p}^2 + m_s v_s^2 \\ m_p v_{i,p} &= m_p v_{f,p} \cos \theta + m_s v_s \cos \phi \\ 0 &= m_p v_{f,p} \sin \theta - m_s v_s \sin \phi \end{aligned} \quad (1)$$

Here the subscripts i and f denote initial and final states respectively and p and s denote projectile and sample particles respectively. Before continuing the reader should be aware of two different types of ion scattering as illustrated in figure 1.

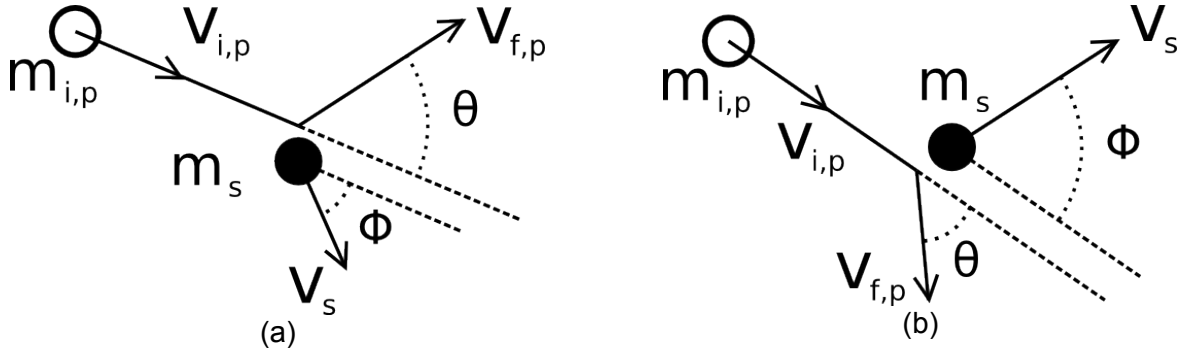


Figure 1: (a) reflection and (b) recoil. For clarity there is only one atom of the sample drawn, in both cases the sample is made up of more atoms on and below the horizontal line through the single sample atom drawn.

The theoretical velocities of these particles can be found by combining formulas (1) and thereby eliminating either v_s and ϕ or $v_{f,p}$ and θ [5]. There are multiple ways of arriving at the same results, a more detailed explanation is given in [3] among others.

$$v_{ref} = v_{i,p} \frac{\cos \theta \pm \sqrt{\mu^2 - \sin^2 \theta}}{1 + \mu} \quad (2)$$

$$v_{rec} = 2 v_{i,p} \frac{\cos \phi}{1 + \mu} \quad (3)$$

Here $\mu = m_s / m_p$, the plus sign in (2) is only valid when $\mu > 1$, both plus and minus are valid for $1 > \mu > \sin \theta$. In the other cases equation (2) with the minus sign corresponds to an unphysical situation with a negative velocity. In an ISS experiment all the variables in (2) and (3) except the

mass of the target atom are known. Thus the mass of the target atom can be determined. Depending on whether reflected or recoiled particles are measured one usually refers to this technique as respectively Low Energy Ion Scattering (LEIS) [5] or Low Energy Recoil Scattering (LERS) [4].

2.2 Validity of the classical model

In the past century numerous effects concerning atomic and sub-atomic systems have been found to disagree with classical mechanics. One can expect that these effects also play a role in the scattering of atomic particles and thus that the classical model is incorrect. However, within the terms of LEIS and LERS these effects are negligible as some calculations on extreme cases will show.

With LEIS and LERS energies of up to tens of keV are used. In the extreme case of a $100keV$ helium beam velocities of about $2.3 * 10^6 m s^{-1}$ will be achieved which is still only 0.7% of the speed of light so relativistic effects can be neglected.

Typical thermal vibrations have a period of about $10^{-12} - 10^{-13} s$ where collisions times are about $10^{-15} s$ so during a collision it will seem as if the sample atoms are standing still [6]. This also means there is no transfer of thermal energy.

The periodic crystal lattice of the sample can cause a diffraction effect. This will happen if the de Broglie wavelength of the projectile is in the same order of magnitude as the inter-atomic distance of the sample. Typical inter-atomic distances are in the order of $10^{-10} m$, the de Broglie wavelength will be at least a factor 10 larger for $1 eV$ He^+ projectiles and will become even larger for increasing momentum. It can be concluded that diffraction is also negligible.

3. Experimental setup

Like most of the setups at ATF, IISIS also relies on the Electron Cyclotron Resonance Ion Source (ECRIS) for its highly charged ions. The ions coming from the ECRIS are guided through a central beamline and can be directed to the different setups by means of 45° bending magnets. Because ions with charge q coming from ECRIS have a minimum energy of about $3q \text{ keV}$ they need to be decelerated when a measurement calls for sub $3q \text{ keV}$ ions. Therefore the whole setup including pumps and electronics can be floated on high potential, an electrostatic lens system is installed to focus the beam.

Inside the chamber the pressure is brought down into the low 10^{-9} mbar regime. For measurements of LEIS/LEIS velocities a Time Of Flight (TOF) tube with channeltron is attached. The important parts are described in more detail in the following sections.

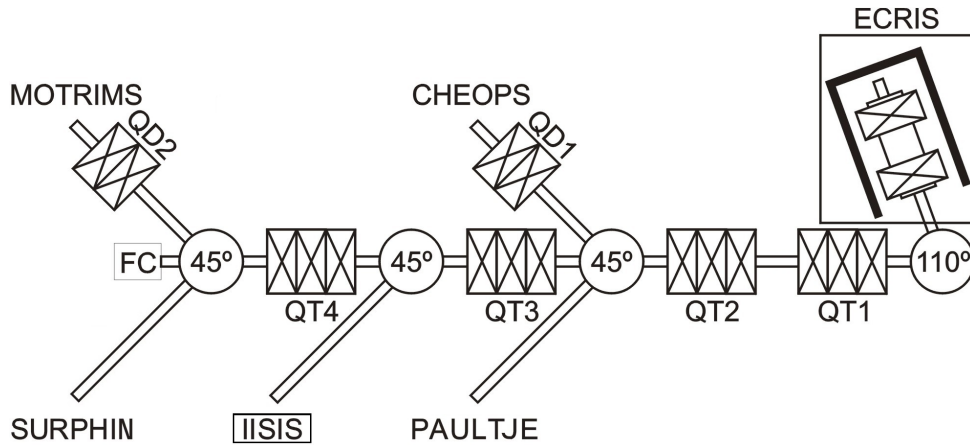


Figure 2: Overview of the ATF lab. Original image from [1], modified by Adrian de Nijs.

3.1 Vacuum chamber

The chamber is made out of a standard stainless steel CF 150 six way cross. A 360 l/s turbo pump is attached to bring the pressure down during bake-out. During the bake-out process the sample can be heated with the aid of a heating element capable of reaching temperatures up to 400°C . To keep the system at a pressure of 10^{-9} mbar a 400 l/s ion getter pump is used [7].

The sample manipulator has three translational degrees of freedom. Two degrees are in the horizontal plane both allowing the sample to travel $\pm 12.5 \text{ mm}$. The vertical degree has a maximum travel of 150 mm . The sample can also be rotated by 360° . For the duration of this research a gold sample was used.

The sample is electrically isolated from the system. A connection is available to measure the current produced by the ion beam on the sample. Opposite the entrance of the ion beam is a faraday cup to measure the current when the sample is not in the beam path.

For the creation of a thin film on the sample an evaporator filled with C_{60} is installed. This can also be used as a test for the TOF system: When in between two measurements some C_{60} is evaporated onto the sample a clear difference in the results should be visible.

For the electron yield measurements a Surface Barrier Detector (SBD) placed at a 90° angle with respect to the ion beam entering the chamber is used. The sample is surrounded by six electrodes used to maximize the yield onto the SBD. One electrode consists of a grid placed in front of the

SBD, the grid is put on positive potential so to attract electrons toward the SBD. The other five electrodes are either plates or grids which are put on a negative potential thereby repelling the electrons toward the SBD.

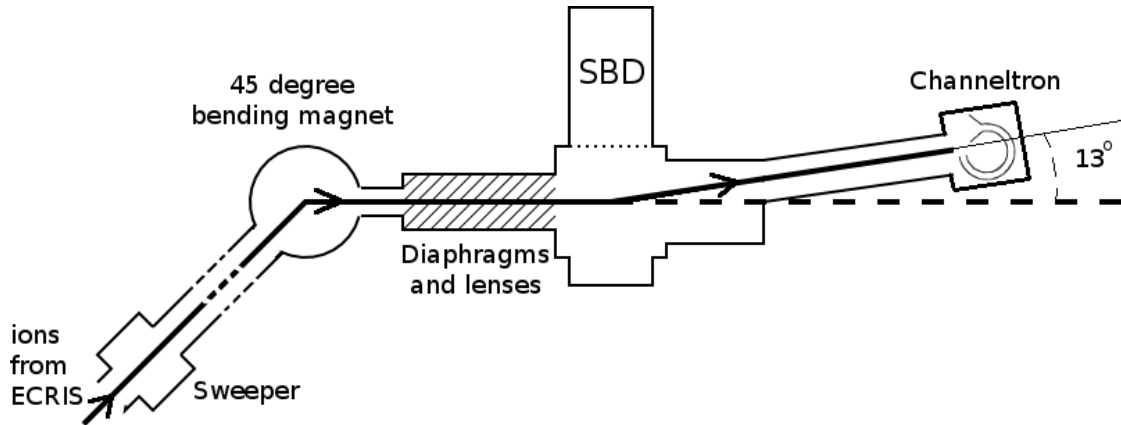


Figure 3: Schematic top view of ISIS. Some parts, like pumps and grids, are left out for clarity.

3.2 Deceleration

The kinetic energy of the ions coming from ECRIS is determined by the source potential V_{Source} and the plasma potential $V_{Plasma} = 15 \pm 10 V$. The kinetic energy is given by $E_{Kin} = q(V_{Source} + V_{Plasma})$. In order to decelerate the ions the whole setup including pumps and electronics is brought to a potential V_{Setup} , this makes for the ions when reaching the sample to have a kinetic energy of $E_{Kin} = q(V_{Source} + V_{Plasma} - V_{Setup})$. V_{Setup} needs to be defined properly with respect to V_{Source} in order to prevent fluctuations between V_{Source} and V_{Setup} . This is achieved by floating the whole setup on the source potential in series with a high voltage power supply providing a bias potential V_{Bias} , figure 4 illustrates this. With this configuration we have for the kinetic energy of the ions entering the chamber of IISIS:

$$\begin{aligned} E_{Kin} &= q(V_{Source} + V_{Plasma} - V_{Setup}) \\ &= q(V_{Source} + V_{Plasma} - (V_{Source} - V_{Bias})) \\ &= q(V_{Plasma} + V_{Bias}) \end{aligned}$$

This way the total kinetic energy of an ion reaching the sample is determined only by a controllable bias potential and a small plasma potential.

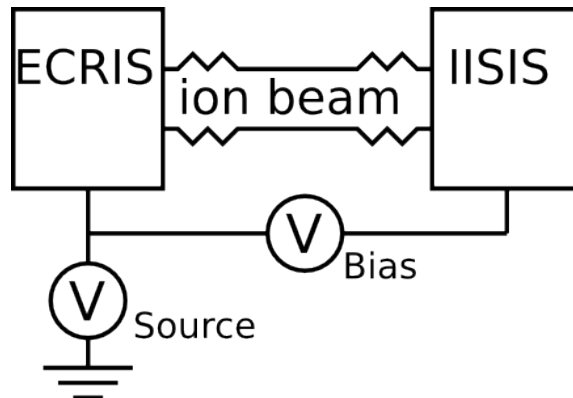


Figure 4: Schematic diagram of the potentials determining the final ion beam energy. The plasma potential is left out.

The deceleration of the ion beam has the unwanted effect of diverging it, therefore an electrostatic lens system is installed. The electrostatic lens system consists of four metal cylinders with the beampath on the central axes. Between the cylinders there is a small gap. With a different potential on two neighboring cylinders a potential gradient will exist in the region of the gap, this gradient works just like an optical lens [2].

The path of ions through such a lens system can be simulated with computer programs like Simlon. With such a program the performance of the lens system gets much clearer and a lot of different settings can be tried quickly.

3.3 Time of flight

The TOF tube is attached under a fixed angle of 13° with respect to the ion beam entering the chamber. The distance from the center of the chamber to the particle detector is $764 \pm 1 \text{ mm}$. In this setup a channeltron is used as the particle detector. The last $421 \pm 1 \text{ mm}$ of the TOF tube is fitted with an electrically isolated inner tube which can be put on high potential. This can be used to separate the ions from the neutralized particles.

A pair of horizontally placed sweeper plates is mounted before the 45° bending magnets so that the distance from the plates to the center of the chamber is $4.0 \pm 0.2 \text{ m}$. The sweeper plates are used to make ion packets from the continuous beam. This is done by applying a square wave potential with its top at u_1 and a period p to one of the plates. The other plate is put on a fixed potential of $u_2 < u_1$. This will cause the ion beam to be swept in the vertical direction over the first diaphragm after the sweeper plates. The beam direction is unchanged whenever the potential on both plates is equal, at that moment the beam passes straight through the diaphragm.

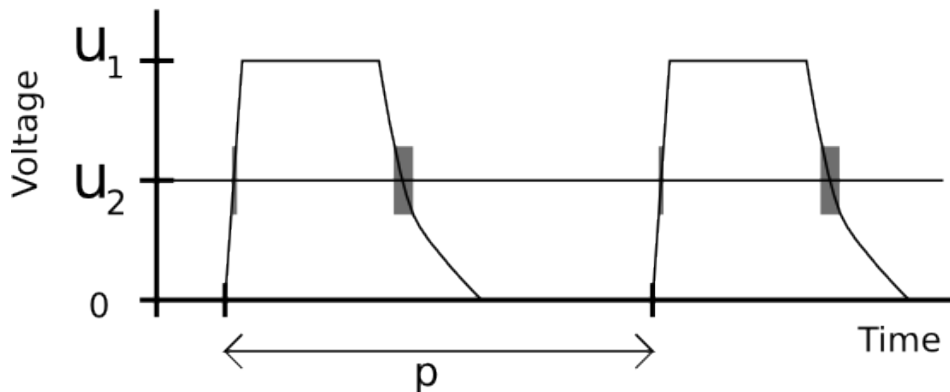


Figure 5: Voltages put on the sweeper plates.

The falling flank is much slower compared to the rising flank, the difference between the two packets is illustrated by the gray areas in figure 5. The width of the gray area on the rising flank is shorter, signifying a shorter packet. One of both packets may be chopped out with an additional pair of plates but those are not available in the current setup, yet. Other things that influence the length of the packets are the dimensions of the sweeper plates and the radius of the diaphragm after the plates. However, these dimensions are unknown. So the length of the packets can not be calculated and has to be determined experimentally.

A computer equipped with a Time to Digital Converter (TDC) is used for the actual measurement of the TOF spectrum. The TDC is a P7888 which together with the appropriate software is supplied by Fast ComTec.

The TDC takes two inputs: A trigger signal and the channeltron signal. The trigger signal is used to start the TDC. The time difference between the trigger signal and a pulse of the channeltron is logged for every channeltron pulse i.e. for every detected particle. The maximum resolution or binwidth is 1 ns .

3.4 LEIS or LERS?

The flight distance and the total scattering angle are both fixed but there are still a number of variables which can be chosen as to optimize the results. The goal will be to get a significant difference in flight times of the expected elements. This is particularly useful for the first measurements when the settings probably are not optimal yet. When it is proven the setup works other conditions can be chosen and parameters influencing peak widths can be optimized.

With the ECRIS a plethora of elements can be ionized and accelerated. Preferably either helium, neon or argon ions will be used because at ATF there is a lot of experience with these. An added advantage is that these ions leave little contamination on the sample.

Carbon and oxygen are well known contaminations when working in UHV. Also the detection of carbon is important for the planned experiments on gold covered with layers of C₆₀. Theoretical flight times of these elements are summarized in table 1. These are calculated for ion beams with an energy of $7q\text{ keV}$ and a total scattering angle of 13° . It should be noted that these flight times do not include the flight time from sweeper to sample.

	Argon			Neon			Helium		
	LERS	+ LEIS	-	LERS	+ LEIS	-	LERS	+ LEIS	-
¹² C	2785	4627	*	2423	3085	11294	2709	1331	*
¹⁶ O	2999	4478	*	2726	3050	25709	3387	1328	*
¹⁹⁷ Au	12691	4196	*	16433	2959	*	34036	1321	*

Table 1: Theoretical flight times in ns from sample to detector for various situations using $7q\text{ keV}$ ions (* indicates an unphysical situation).

Helium being very light has little chance of recoiling an atom from the surface. Therefore LEIS will produce the most significant peaks. As can be seen from table 1 the LEIS flight times are all within 20 ns , it will turn out this is well within the peak width so it is impossible to distinguish individual peaks.

Theoretically it should be possible to decelerate the helium ions to $10q\text{ eV}$. However, since the sweeper system including the measuring computer is also used for other projects at ATF it is not possible to bring IISIS up to the high potential needed for deceleration yet. To find out whether it is worth solving this situation the LEIS flight times for helium ions with an energy of $10q\text{ eV}$ are summarized in table 2.

	Helium		
	LERS	+ LEIS	-
¹² C	71682	35222	*
¹⁶ O	89602	35147	*
¹⁹⁷ Au	900500	34940	*

Table 2: Theoretical flight times in ns from sample to detector for 10 eV He^+ (* indicates an unphysical situation).

It can be seen from table 2 that even with very low energy He^+ it will still be difficult to distinguish individual peaks. It is also unlikely that at these low energies the projectile will scatter at all.

Argon seems to be the best choice when considering the distinguishability of peaks. Though, in [4] it becomes clear that this is more difficult compared to helium LEIS. This is because for carbon and oxygen the probability of recoils is small. Making it difficult to get clear results, specially in the early stage of setting up the experiment. Also there seems to be more literature available on LEIS which makes it easier to troubleshoot in case of ambiguities.

4. Measurements

4.1 Deceleration

Several test runs of the deceleration system were done. The current was measured in the faraday cup with and without using the lenses. When the lenses were used they were tuned with the aid of simulations and trial and error to maximize the current. The resulting lens settings were stored to be used for use during electron yield measurements or TOF measurements while decelerating.

Figure 6 (a) and (b) show the results of measurements on two separate days, both roughly have the same shape. As can be seen the deceleration is not of much influence until the ions reach an energy lower than 2.5 keV . With the use of the lenses ion energies of 2.5 keV until 500 eV still provide a current comparable to the undecelerated beam.

For energies below 500 eV a current of about 10% of the undecelerated beam is attainable. Such a current is acceptable, certainly for the electron yield measurements.

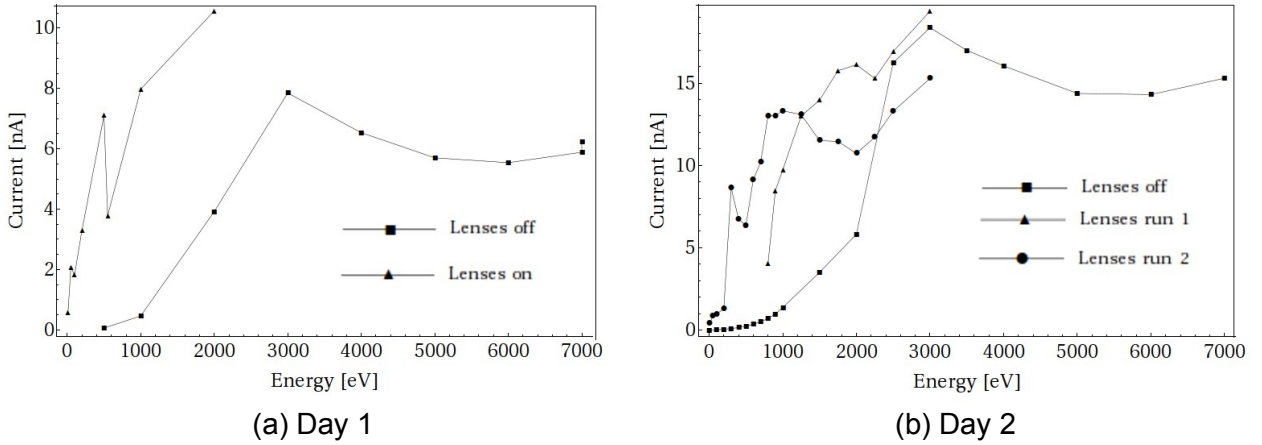


Figure 6: Currents as measured in the Faraday cup of He^+ beams decelerated down from 7 keV with and without focusing of lenses.

4.2 Ion packets

To determine characteristics like packet length and intensity the discontinuous beam was shot directly onto the channeltron with the aid of high voltages on the electrodes. Using Simlon the potentials to aim the beam were roughly determined to be optimized later in practice.

An Ar^+ beam of 7 keV was swiped with the following initial settings on the sweeper plates: a period of $20\text{ }\mu\text{s}$ and a pulse width of $10\text{ }\mu\text{s}$ with $u_1=200\text{ V}$, $u_2=100\text{ V}$. The electrodes were tuned as to get an acceptable count rate on the channeltron, the sample was not in the beam line during these measurements. A measurement was made with a resolution of 2 ns on 9984 channels so one full period is captured, figure 7 shows a plot of the result.

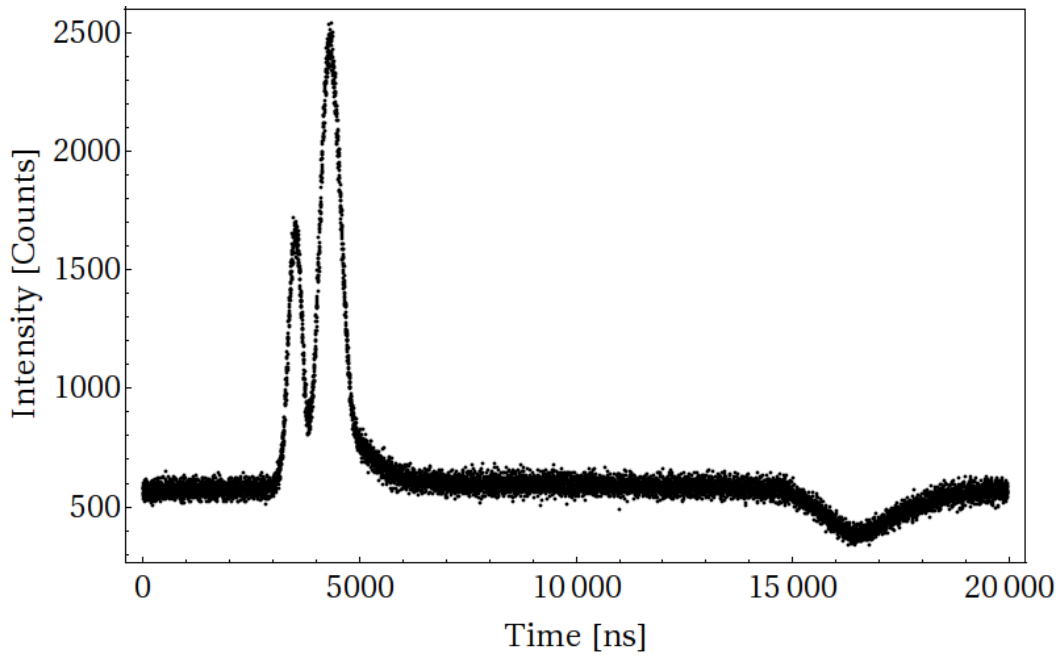


Figure 7: Discontinuous beam directly on channeltron

The time between two packets should be about $10\mu s$ thus the peaks in figure 7 are too close together to be different packets. It is possible that part of a single packet scatters and in that way creates a second beam having a minor deviance in path length. An actual second packet is not visible although there is a minor dip around the place where the second packet is expected, that had to be investigated.

The settings for the beamline and grid proved to be of much influence on the results of the measurement, after several adjustments to the magnets and the grid another peak appeared as shown in figure 8.

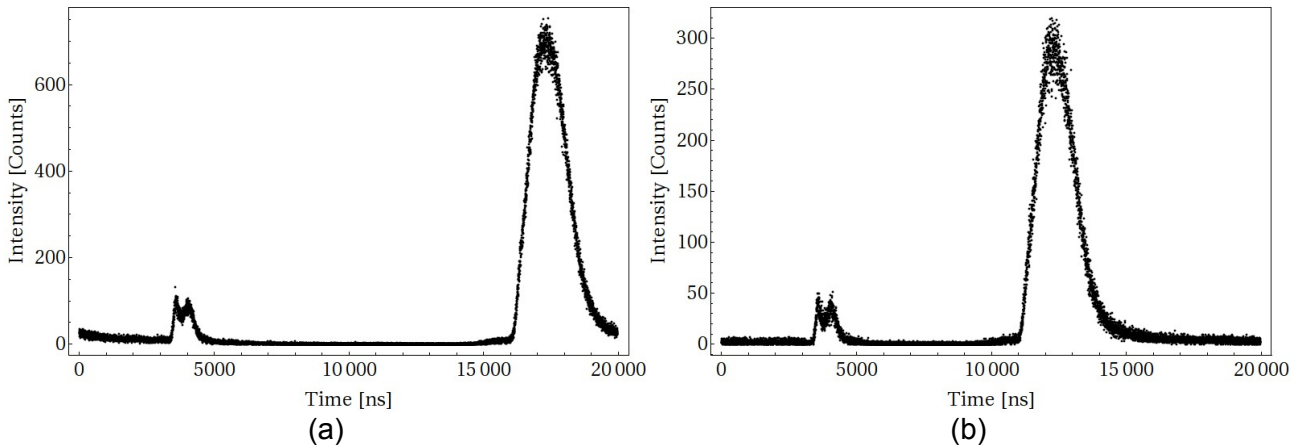


Figure 8 a and b: In b the pulse width on the sweeper plates is brought to $5\mu s$ from $10\mu s$.

The change in time between the two major peaks when the pulse width is changed suggest that there are two packets created by the sweeper plates, one on the rising flank of the square wave and one on the falling flank. The distance between the peaks doesn't correspond exactly with the period set on the pulse generator. A measurement confirmed that the signal going to the sweeper plates does correspond to the time as seen in figure 8 but the period set on the pulse generator is of by about $2\mu s$.

It sometimes happened that while playing with the settings of the electrodes the channeltron registered a very high intensity in the order of 10^7 counts per second. Such high intensities are close to the maximum a channeltron can handle before breaking down thus these measurements couldn't be repeated very often.

One time by chance a measurement was running when the channeltron registered a high intensity and an interesting result was seen, it was repeated under more controlled conditions resulting in figure 9.

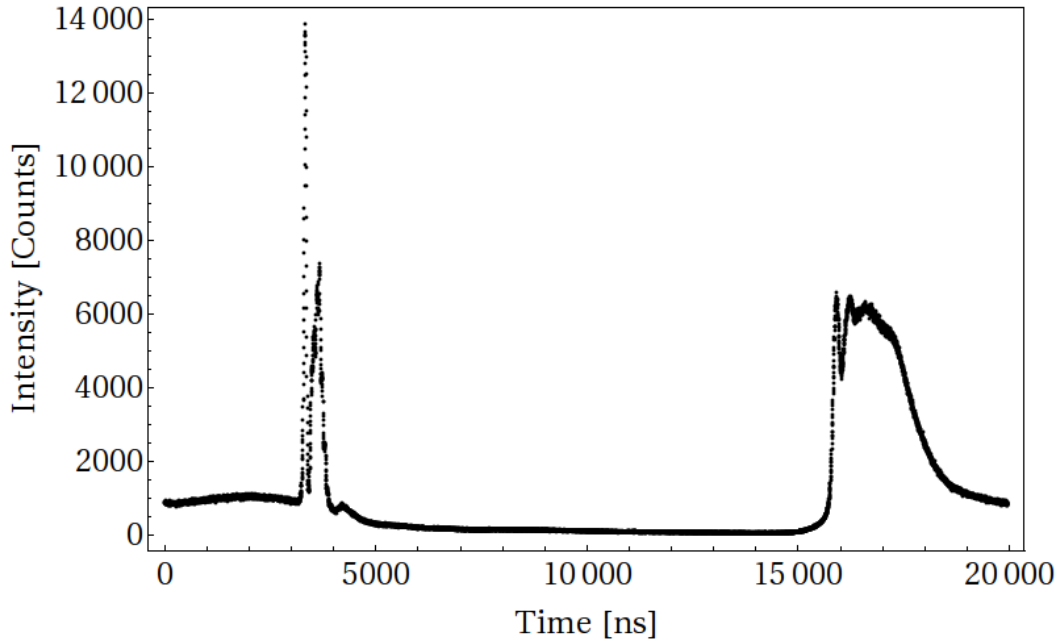


Figure 9: High intensity on channeltron

While the peaks had been pretty broad this far, in the range of microseconds, the first peak in figure 9 shows that the packets are actually fairly short, in the range of 100 ns . The spread in time or better the spread in energy in the other plots is probably due to scattering at one or more diaphragms. There still remains the question of the double peaks structure though.

Further research was done on the variables influencing the peak width. Considering the shape of the square wave on the sweeper plates (Figure 5) it was expected that the peak width would go down when the constant voltage u_2 on the sweeper plates was closer to the top u_1 of the square wave. Table 3 summarizes the results where it can be clearly seen that the potential on the sweeper plates affects the width of the peak.

u_1	u_2	Width
200 V	100 V	3200 ns
200 V	150 V	1800 ns
200 V	175 V	1700 ns

Table 3: The peak width depends on the height of u_2 .

5. Conclusion

The configuration of the deceleration system gave little problems. The simulations were a good guide to find the optimal settings. With the gathered settings it should be easy to configure the lenses when they are needed in the future.

The Time Of Flight (TOF) system proved to not be ready for serious use yet. Numerous measurements were made but results were hardly reproducible. One of the main issues was the dependence on minor adjustments to the correction magnets. That suggests that if the sweeper system is moved to a place after the 45° bending magnet better results will be obtained.

In the current setup a sweeping ion beam has to travel through a correction magnet and a 45° bending magnet before passing a diaphragm. It should be no surprise that somewhere along the path the ions scatter in an unexpected way before passing the diaphragm.

Another improvement that can be made is changing the total scattering angle. This is achievable by moving the flange to which the TOF tube is attached by 90° . That way the total scattering angle is 77° . The expected flight times of He^+ from sample to detector for this angle are summarized in table 4.

	Helium		
	LERS	+ LEIS	-
^{12}C	11735	1724	*
^{16}O	14669	1608	*
^{197}Au	147425	1341	*

Table 4: Theoretical flight times in ns from sample to detector for $7\text{ keV } \text{He}^+$ (* indicates an unphysical situation).

As can be seen this way it is possible to do LEIS measurements with helium which are preferred over LERS measurements with argon.

Bibliography

- [1] Danyal Winters, Polarization transfer in ion-surface scattering, PhD thesis RuG 2004
- [2] D.W.O. Heddle, Electrostatic Lens Systems 2d edition, IoP
- [3] H. Goldstein, Classical Mechanics 2d edition, Addison Wesley
- [4] S.J. Doornenbal, Determination of adsorbate coverages on surfaces with low energy recoil scattering, PhD thesis RuG 1994
- [5] H. Niehus, W. Heiland and E. Taglauer, Surf. Sci. Rep. 17 (1993) 213
- [6] J.C. Vickerman, I.S. Gilmore, Surface analysis The principal techniques, Wiley
- [7] E. Bodewits, (unfinished at the time of writing) PdD thesis RuG
- [8] Retrieved from: <http://www.geocities.com/athens/2962/colourbook/isis2.gif> on 16/07/2009, modified by Hendrik Bekker